Prescribed Performance Tracking of a Variable Stiffness Actuated Robot

Efi Psomopoulou, *Student Member, IEEE,* Achilles Theodorakopoulos, *Student Member, IEEE,* Zoe Doulgeri, *Member, IEEE,* and George A. Rovithakis, *Senior Member, IEEE*

***Abstract*—This paper is concerned with the design of a state feedback control scheme for variable stiffness actuated (VSA) robots, which guarantees prescribed performance of the tracking errors despite the low range of mechanical stiffness. The controller does not assume knowledge of the actual system dynamics nor it utilizes approximating structures (e.g., neural networks, fuzzy systems) to acquire such knowledge, leading to a low complexity design. Simulation studies, incorporating a model validated on data from an actual VSA at a multi-dof robot, are performed. Comparison with a gain scheduling solution reveals the superiority of the proposed scheme with respect to performance and robustness.**

I. Introduction

THE introduction of robots in human everyday activities for service and assistance at both home and work, has motivated a series of new developments seeking to address the issues of safety and performance, in human-robot co-existence.

An approach to resolve concurrently safety and performance issues is via the design and development of variable stiffness actuators (VSA), which introduce a mechanical compliance in the joint actuation that can be altered via control action [1]–[7]. The greater complexity of the mechanical designs and the coupling of actuators responsible for adjusting simultaneously joint position and stiffness has introduced serious technical issues related to controller design. Initial attempts have concentrated in feedback linearization solutions that require extensive model knowledge or identification to achieve satisfactory operation [8]–[13]. Impedance and damping control for this type of robots has also been investigated [13], [14]. Recently, gain scheduling strategies have been proposed for achieving robustness to stiffness parameter variations of VSA of the antagonistic or series type [12], [15], leaving however open the problem of extending their control designs to multi dof robots.

To our knowledge, all current control approaches assume a given task-related desired stiffness profile that reflects damage or injury risk assessment in the event of collision; for example, higher velocities are typically associated with low stiffness profiles so that in case of impact, the risk of damage or human injuries is reduced [16]. At the same time, low stiffness is reported to yield large tracking errors, which in turn may also be the source of collisions in an uncertain and dynamic environment [15]. Moreover, by increasing mechanical stiffness, performance is not necessarily guaranteed.

In this work, prescribed performance of the tracking error in the presence of low joint stiffness is achieved, via the utilization of a controller developed for a variable stiffness joint of a series type [17] that is here extended to the multi dof case. It is assumed that in case of impact, a practical remedy could be the prescribed performance controller to be deactivated, leaving the robot under the control of online gravity compensation with joint damping. It is stressed that prescribed performance is achieved without incorporating the actual robot-motor dynamics and without depending on approximating structures (e.g., neural networks, fuzzy systems) to acquire such knowledge, thus resulting in a low complexity control design. Simulation results for a multi dof robot, incorporating the recently developed model [3] that was validated on data obtained from an actual VSA joint, are included. We move forward and conduct simulations comparing our approach to the gain scheduling solution [15].

The paper is organised as follows: in Section II the main problem addressed is stated, while in Section III the proposed controller is presented. Simulation studies, including comparisons, are conducted in Section IV. Finally, we conclude in Section V. In Appendix A preliminaries on the Prescribed Performance Control methodology is provided, while Appendix B contains technical details related to the stability analysis of the proposed control scheme.

II. Problem Description

Let us consider a $n-$link flexible joint robot with variable stiffness actuators (VSA) consisting of two modules, the stiffness actuator module which regulates the stiffness and the position actuator module which regulates the joint's link position. A reduced model of the aforementioned system can be expressed as follows [3], [15]:

$$M(q)\ddot{q} + C(q,\dot{q})\dot{q} + G(q) = K(\theta_k)(\theta - q) \quad (1)$$

$$J_\theta\ddot{\theta} + B_\theta\dot{\theta} + K(\theta_k)(\theta - q) = \tau_m \quad (2)$$

$$J_k\ddot{\theta}_k + B_k\dot{\theta}_k + F(\theta, q, \theta_k) = \tau_k \quad (3)$$

where $q \in \mathbb{R}^n$ are the link angles, $\theta \in \mathbb{R}^n$ are the link motor angular positions, $\theta_k \in \mathbb{R}^n$ are the stiffness motor angular

This research is co-financed by the EU-ESF and Greek national funds through the Operational Program "Education and Lifelong Learning" of the National Strategic Reference Framework (NSRF)-Research Funding Program ARISTEIA I

The work of A. Theodorakopoulos was supported by the IKY Fellowships of Excellence for Postgraduate Studies in Greece Siemens Program, Greek State Scholarships Foundation.

The authors are with the Department of Electrical and Computer Engineering, Aristotle University of Thessaloniki, 54124 Thessaloniki, Greece. emails: efipsom@ee.auth.gr, konstheo@eng.auth.gr, doulgeri@eng.auth.gr, robi@eng.auth.gr

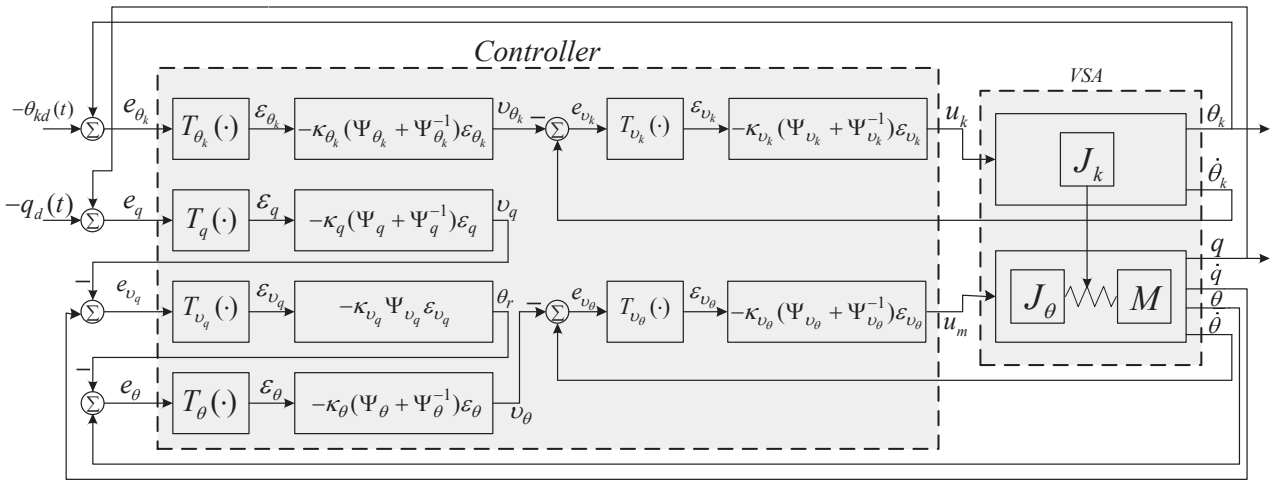

Fig. 2. The proposed control scheme.

positions, while $\dot{q}, \dot{\theta}, \dot{\theta}_k \in \mathbb{R}^n$ are the respective velocities. Moreover, $M(q) \in \mathbb{R}^{n\times n}$ is the link side inertia matrix, $C(q,\dot{q}) \in \mathbb{R}^{n\times n}$ is the Coriolis/centrifugal matrix, $G(q) \in \mathbb{R}^n$ is the gravity vector, $J_\theta, J_k \in \mathbb{R}^{n\times n}$ are the two motor diagonal, positive definite inertia matrices and $B_\theta, B_k \in \mathbb{R}^{n\times n}$ are the motor damping matrices, including both the physical damping and back emf damping of the motors. Moreover, $K(\theta_k) \in \mathbb{R}^{n\times n}$ is a diagonal joint stiffness matrix with entries $K_i(\theta_{k_i}), i = 1,\dots,n$ and $F(\theta,k,\theta_k) \in \mathbb{R}^n$ is a vector with nonlinear entries $F_i(\theta_i, q_i, \theta_{k_i}), i = 1,\dots,n$, representing the reaction torques produced by the deflection of the elastic transmission that act against the motor adjusting the stiffness. A schematic of the actuator model and operation principle of one joint is shown in Fig. 1. The entries $K_i(\theta_{k_i}), i = 1,\dots,n$ of

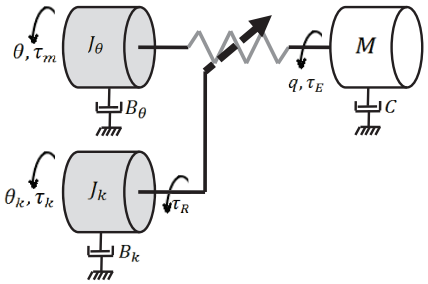

Fig. 1. Schematic of the actuator model and operation principle.

the joint stiffness matrix $K(\theta_k)$ are strictly positive, bounded, continuous functions of θ_k, that are not necessarily equal. It is considered

$$K_i(\theta_{k_i}) \geq k_i > 0, \forall t \geq 0, i = 1,\dots,n \tag{4}$$

where k_i possibly small constants. This is imposed by construction and low level firmware limits [3] and is required to establish a well-defined joint stiffness representation as well as a controllable VSA model (1)-(3). Finally, assuming ideal motor transmissions with negligible internal losses, $\tau_m, \tau_k \in \mathbb{R}^n$ are the motor torques after the reduction drives which are given by $\tau_m = K_\theta u_m$, $\tau_k = K_k u_k$ where u_m, u_k are the input voltages vectors and K_θ, K_k are positive definite constant diagonal matrices.

Following its definition, the joint stiffness matrix $K(\theta_k)$ can be decomposed, without losing generality, as

$$K(\theta_k) = K_M(\theta_k)\,\mathcal{I} + \Delta K(\theta_k) \tag{5}$$

where $K_M(\theta_k) > 0$ is an unknown, continuous and bounded function of θ_k, defined as

$$K_M(\theta_k) = \max_i \{K_i(\theta_k)\},\ i = 1,\dots,n, \tag{6}$$

$\mathcal{I}$ is the $n \times n$ identity matrix and $\Delta K(\theta_k)$ is an unknown though bounded $n \times n$ diagonal matrix. The matrix $\Delta K(\theta_k)$ introduces the required diversity in the elements of $K(\theta_k)$. The special case where $\Delta K(\theta_k) = 0, \forall \theta_k > 0$ applies to a manipulator possessing identical joint stiffnesses.

For the VSA system (1)-(4), the state $x = (q, \dot{q}, \theta, \dot{\theta}, \theta_k, \dot{\theta}_k)$, is assumed to be available for measurement, while its dynamics is assumed to be unknown.

Our goal is to design a state feedback controller to control the outputs $q, \theta_k \in \mathbb{R}^n$ of the flexible joint robot with variable stiffness joints to track a given, C^1 and bounded reference trajectory $q_d(t) \in \mathbb{R}^n$, $\theta_{kd}(t) \in \mathbb{R}^n$ respectively, with prescribed performance. This means that the output error should be guaranteed to converge to a predefined arbitrarily small residual set, with rate less than a prespecified value, exhibiting maximum overshoot less than a sufficiently small preassigned constant. Moreover, all other closed loop signals should be kept bounded. The above task shall be referred to as the *Prescribed Performance Control for a Variable Stiffness Actuator Robot (PPC/VSA) problem.*

III. Controller Design

Let us define $\varepsilon_j,\ j \in \{q, v_q, \theta, v_\theta, \theta_k, v_k\}$ as

$$\varepsilon_j = \left[T_{j1}\left(\frac{e_{j1}}{\rho_{j1}}\right)\ \dots\ T_{jn}\left(\frac{e_{jn}}{\rho_{jn}}\right)\right]^{\mathsf{T}} \in \mathbb{R}^n, \tag{7}$$

with $e_q = q - q_d \in \mathbb{R}^n, e_{\theta_k} = \theta_k - \theta_{kd} \in \mathbb{R}^n, e_{v_q} = \dot{q} - v_q \in \mathbb{R}^n, e_\theta = \theta - \theta_r \in \mathbb{R}^n, e_{v_\theta} = \dot{\theta} - v_\theta \in \mathbb{R}^n, e_{v_k} = \dot{\theta}_k - v_{\theta_k} \in \mathbb{R}^n$ and $\rho_{ji},\ j \in \{q, v_q, \theta, v_\theta, \theta_k, v_k\},\ i = 1, \ldots, n$ are performance functions defined in the Prescribed Performance Preliminaries provided in Appendix A. Moreover, $v_q, \theta_r, v_\theta, v_{\theta_k}$ are intermediate control signals and

$$\Psi_j = \text{diag}\left[\frac{1}{\rho_{ji}} \frac{\partial T_{ji}}{\partial \left(\frac{e_{ji}}{\rho_{ji}}\right)}\right] \in \mathbb{R}^{n \times n}, \tag{8}$$

$j \in \{q, v_q, \theta, v_\theta, \theta_k, v_k\},\ i = 1, \ldots, n$. Notice that $\Psi_j > 0$. In the derivation of (8) any transformation function T_{ji} satisfying the properties stated in the Prescribed Performance Preliminaries provided in Appendix A can be utilized, as for example (19). A solution to the considered problem, is provided by

$$u_m(t) = -\kappa_{v_\theta}\left(\Psi_{v_\theta} + \Psi_{v_\theta}^{-1}\right)\varepsilon_{v_\theta} \tag{9}$$

$$v_\theta(t) = -\kappa_\theta\left(\Psi_\theta + \Psi_\theta^{-1}\right)\varepsilon_\theta \tag{10}$$

$$\theta_r(t) = -\kappa_{v_q}\Psi_{v_q}\varepsilon_{v_q} \tag{11}$$

$$v_q(t) = -\kappa_q\left(\Psi_q + \Psi_q^{-1}\right)\varepsilon_q \tag{12}$$

$$u_k(t) = -\kappa_{v_k}\left(\Psi_{v_k} + \Psi_{v_k}^{-1}\right)\varepsilon_{v_k} \tag{13}$$

$$v_{\theta_k}(t) = -\kappa_{\theta_k}\left(\Psi_{\theta_k} + \Psi_{\theta_k}^{-1}\right)\varepsilon_{\theta_k} \tag{14}$$

where, in (9)-(14), $\kappa_j,\ j \in \{q, v_q, \theta, v_\theta, \theta_k, v_k\}$ are positive control gains. Fig. 2 illustrates the proposed control scheme. The following theorem summarizes the main results of the paper.

Theorem 1: Consider a n-link flexible joint robot with variable stiffness actuators (1)-(4) and desired bounded and C^1 tracking trajectories $q_d(t), \theta_{kd}(t)$. Further, consider a set of performance functions $\rho_{ji}(t),\ j \in \{q, v_q, \theta, v_\theta, \theta_k, v_k\}, i = 1, \ldots, n$ and constants M_{ji} satisfying $0 \leq M_{ji} \leq 1,\ j \in \{q, v_q, \theta, v_\theta, \theta_k, v_k\}, i = 1, \ldots, n$ which incorporate desired performance characteristics on the corresponding errors $e_{ji}(t)$, $j \in \{q, v_q, \theta, v_\theta, \theta_k, v_k\}, i = 1, \ldots, n$. The prescribed performance controller (7)-(14) with transformation functions

$$T_{ji}\left(\frac{e_{ji}(t)}{\rho_{ji}(t)}\right) = \begin{cases} a_{ji} \ln\left(\frac{M_{ji} + \frac{e_{ji}(t)}{\rho_{ji}(t)}}{1 - \frac{e_{ji}(t)}{\rho_{ji}(t)}}\right), \text{in case } e_{ji}(0) \geq 0 \\ a_{ji} \ln\left(\frac{1 + \frac{e_{ji}(t)}{\rho_{ji}(t)}}{M_{ji} - \frac{e_{ji}(t)}{\rho_{ji}(t)}}\right), \text{in case } e_{ji}(0) \leq 0 \end{cases}$$

where $a_{ji} > 0,\ j \in \{q, v_q, \theta, v_\theta, \theta_k, v_k\}, i = 1, \ldots, n,\ \kappa_j,$ $j \in \{q, v_q, \theta, v_\theta, \theta_k, v_k\}$ positive design constants and

$$|e_{ji}(0)| < \rho_{ji}(0) \quad , \quad if\ e_{ji}(0) \neq 0$$
$$M_{ji} \neq 0 \quad , \quad if\ e_{ji}(0) = 0$$

with $j \in \{q, v_q, \theta, v_\theta, \theta_k, v_k\}, i = 1, \ldots, n$ solves the PPC/VSA problem.

Proof. For completeness and compactness of presentation, the proof of Theorem 1, which is strongly influenced by [18], is provided in Appendix B. □

The proposed controller achieves prescribed performance requirements for the system output error (e_q, e_{θ_k}) regarding the maximum steady state error, the minimum speed of convergence as well as the maximum overshoot using state feedback and without requesting any knowledge of the system nonlinearities. Furthermore, neither adaptive techniques nor approximating structures i.e., neural fuzzy systems etc., are utilized to acquire such knowledge or compensate for its absence. Thus, the controller summarized in Theorem 1 is the simplest architecture reported in the relevant literature capable of succeeding such a demanding task for a multi-dof variable stiffness actuator robot.

It is noted however that the proposed controller does not guarantee the quality of output error evolution inside the performance envelope[1] defined by the output performance functions $\rho_{qi}(t),\ \rho_{\theta_k i}(t),\ i = 1, \ldots, n$ and constants M_{qi}, $M_{\theta_k i}, i = 1, \ldots, n$. Nevertheless, extensive simulation studies revealed that the selection of the remaining control elements i.e., $\rho_{ji}(t), M_{ji}, k_j, T_{ji},\ j \in \{v_q, \theta, v_\theta, v_k\},\ i = 1, \ldots, n$ can have positive influence. Therefore, the selection of the aforementioned elements should be performed in the direction of establishing smooth output tracking error evolution with reasonable control effort in terms of magnitude and slew rate. It is stressed, however, that currently no universal procedure exists to achieve such a parameter tuning, with the latter being heavily dependent on the application.

Perhaps the strongest limitation of applying the Prescribed Performance Control methodology to a real robot is related to the actuator specifications with respect to the intended prescribed performance of the closed-loop system. As all actuator systems, depending on their construction, are characterized by a maximum delivered torque and a maximum speed of response (bandwidth), it is important to prescribe a closed-loop system performance that for a given control parameters selection can be realized by those actuators. In the opposite case, it is possible that the demanded torque is saturated or delivered in a slower rate than required, causing the performance of the closed-loop system to deteriorate and even to jeopardize stability. It is understood that further research is required in this direction to provide a theoretically justified, viable solution. Fortunately, the feasibility of the aforementioned endeavour is supported by recently reported works that include implementations of the Prescribed Performance Control methodology to visual servoing [19], control of rigid robots [20]–[24], control of underwater vehicles [25], [26] and control of aerial vehicles [27].

IV. Simulation Studies

To demonstrate the attributes of the proposed prescribed performance control scheme, a number of simulation studies have been conducted. Specifically, a 3 d.o.f. spatial robotic manipulator with variable stiffness actuators is first considered to verify and clarify the operation of the developed controller. Finally, we proceed further and in Subsection IV-B comparative simulations are presented with a gain scheduling controller that was recently reported to control single-link VSA robots of the class considered in this work. The performed simulations employ the proposed controller in continuous-time, as designed in Section III, without utilizing a discretization algorithm. The latter also holds true for the aforementioned gain scheduling controller.

[1]For an illustration of the performance envelope see Fig. 15 of Appendix A

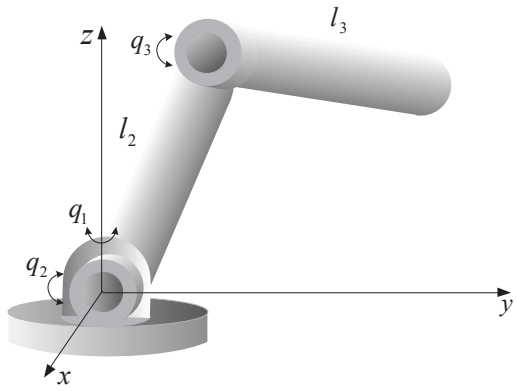

Fig. 3. The 3 d.o.f. spatial robotic manipulator.

A. Simulation study of a 3 d.o.f. VSA robotic manipulator

A 3 d.o.f. spatial robotic manipulator (Fig. 3) is considered with link masses $m_1 = m_2 = m_3 = 1\ kg$, link lengths $l_2 = l_3 = 0.5\ m$ and inertias $I_{z1} = I_{x2} = I_{x3} = 4.15 \cdot 10^{-4}\ kgm^2$, $I_{y2} = I_{z2} = 0.021\ kgm^2$ and $I_{y3} = I_{z3} = 0.0039\ kgm^2$. At each joint, the actual compact variable stiffness actuator [3], [17] is used. Its mathematical description is governed by (2), (3) with joint stiffness matrix entries $K_i(\theta_{ki})$ and reaction torque entries $F_i(\theta_i, q_i, \theta_{ki})$ given as follows:

$$\begin{aligned} K_i(\theta_{ki}) &= K_{E1} \tfrac{\theta_{ki}^2}{(\Delta - n_1\theta_{ki})^2} \quad , i = 1,2,3 \\ F_i(\theta_i, q_i, \theta_{ki}) &= K_{R1} \tfrac{\theta_{ki}(\theta_i - q_i)^2}{(\Delta - n_1\theta_{ki})^3} \quad , i = 1,2,3 \end{aligned}$$

where $K_{E1} = 1.62 \times 10^{-4}\ N/m^3$, $K_{R1} = 2.43 \times 10^{-6}\ Nm^4$, $\Delta = 0.015\ m$, $n_1 = 0.006\ m/rad$ are construction specific mechanical constants. Also, $J_\theta = 0.0575\ kgm^2$, $J_k = 0.0062\ kgm^2$, $B_\theta = 7.7781\ Nms/rad$, $B_k = 0.5262\ Nms/rad$, $K_\theta = 1.4139\ Nm/V$ and $K_k = 0.6014\ Nm/V$.

The state vector is $x_i = \left[q_i\ \dot{q}_i\ \theta_i\ \dot{\theta}_i\ \theta_{ki}\ \dot{\theta}_{ki}\right]$, $i = 1,2,3$. Our purpose is to force the output $q \in \mathbb{R}^3$ to track a smooth, bounded, third degree desired polynomial trajectory $q_d(t) = q(0) + \big(q(t_f) - q(0)\big)\big(\frac{6}{t_f^5}t^5 - \frac{15}{t_f^4}t^4 + \frac{10}{t_f^3}t^3\big)$ reaching a final desired position $q(t_f)$ at time t_f, while the actuators' stiffness is desired to decrease exponentially at a rate of $e^{-1.8t}$.

For the output errors $e_q(t)$ we require a steady state of no more than 0.01rad and minimum speed of convergence as obtained by the exponential e^{-5t} whereas for the output errors $e_{\theta_k}(t)$ the requirements are 0.01rad and e^{-30t} respectively. Note that the aforementioned specifications have been selected to guarantee that the stiffness motor angle $\theta_k(t)$ reaches its steady state well before the link velocity reaches its maximum value, implying that the stiffness dynamics evolve faster than the link dynamics; thus making the control task even more challenging. As the theoretical analysis dictates, the performance requirements for the rest of the states don't need to be as strict. The aforementioned transient and steady state error bounds are prescribed by setting the parameters M_{ji} appearing in Theorem 1 to unity and using exponential performance functions as defined in (16) (see Appendix A) for all joints. The remaining parameters are provided in Table I. Furthermore, the output and state error transformations are chosen as in (19). The closed loop system was simulated using the control design constants given in Table II. The determination of the aforementioned control parameter values is a serious task that is strongly related to the quality of the closed loop system. Its rigorous solution resides in solving a nonlinear, typically non-convex, multi-objective optimization problem. Traditionally, engineering experience is utilized to provide a heuristic, though practical and typically far from being optimal, solution. As the output error performance bounds are solely determined by performance specifications in the proposed controller, the selection of the controller design constants is made by adopting those values that lead to smooth error evolutions within the respective performance envelopes and to reasonable control efforts with respect to magnitude and slew rate. Besides engineering experience, which is used to provide an initial good guess, gain tuning is achieved herein with the aid of a software tool, developed in our laboratory, which performs the necessary multi-objective optimization via a genetic algorithm approach. The results obtained are sub-optimal, yet of sufficient quality.

TABLE I
PRESCRIBED PERFORMANCE FUNCTION PARAMETERS FOR THE MULTI-DOF CASE

	Joint 1			Joint 2			Joint 3		
	ρ_0	ρ_∞	l	ρ_0	ρ_∞	l	ρ_0	ρ_∞	l
e_q	4	0.01	5	4	0.01	5	4	0.01	5
e_{v_q}	15.5	8.1	0.1	5.7	4.2	15.4	16.7	12	3.4
e_θ	16.8	10.3	5.4	31	30	0.6	20	14.2	14.7
e_{v_θ}	12.5	0.9	14.7	8.3	2.4	6.8	7.2	4.4	13.2
e_{θ_κ}	10	0.01	30	10	0.01	30	10	0.01	30
e_{v_κ}	18.3	8.6	0.1	18	12.8	15.8	15.7	6.3	0.62

TABLE II
CONTROL DESIGN CONSTANTS FOR THE MULTI-DOF CASE

j	κ_j	α_{j1}	α_{j2}	α_{j3}
q	0.2	0.3	0.06	0.72
v_q	1.5	2.67	9.18	2.27
θ	0.3	1.9	2.95	3.2
v_θ	0.4	3.35	3.2	9.5
θ_κ	0.4	0.25	0.2	0.15
v_κ	45	0.8	2.7	0.4

We initialize at $\theta_{ki} = 2.175\ rad$, $q_1 = q_3 = 0\ rad$, $q_2 = 1.5708\ rad$ while having zero velocities and deflections ($\theta_i - q_i$, $i = 1,2,3$). The final desired link position is $q(t_f) = [-1.12\ 0.4508\ 1.12]^T\ (rad)$ with $t_f = 6$ sec.

The simulation results are depicted in Figs. 4-9. Specifically, Figs. 4-6 show the link, motor angles and velocities evolution. The stiffness evolution of all joints is pictured in Fig. 7 which starts from a value of $200\ Nm/rad$ decreasing to a value of $100\ Nm/rad$. Apparently, the output errors clearly satisfy the prescribed performance specifications as illustrated in Fig. 8. It is stressed that their magnitude at steady state is 10^{-3} and 10^{-7} for $e_q(t)$ and $e_{\theta_k}(t)$ respectively. Finally, the requested control effort (input torques) is illustrated in Fig. 9. Clearly, the control effort is reasonable for such a demanding control task.

The aforementioned simulations were conducted assuming

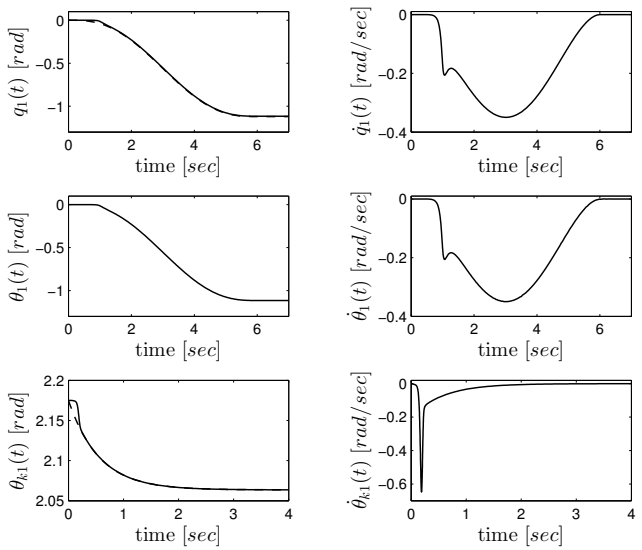

Fig. 4. Time evolution of the link, motor angles and velocities for the first joint alongside their references (dashed lines).

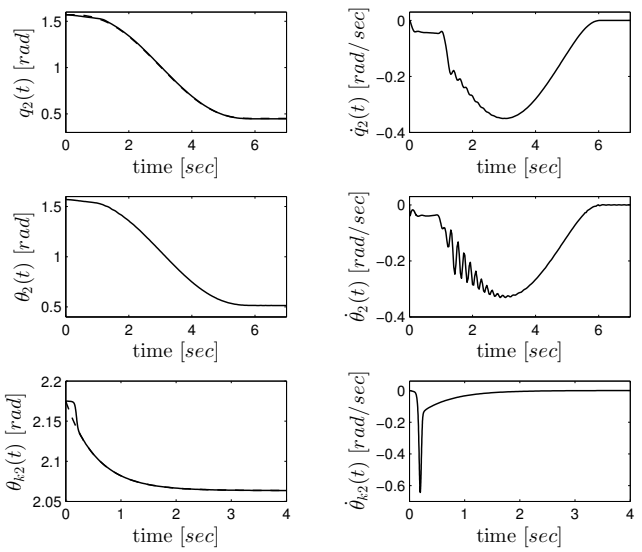

Fig. 5. Time evolution of the link, motor angles and velocities for the second joint alongside their references (dashed lines).

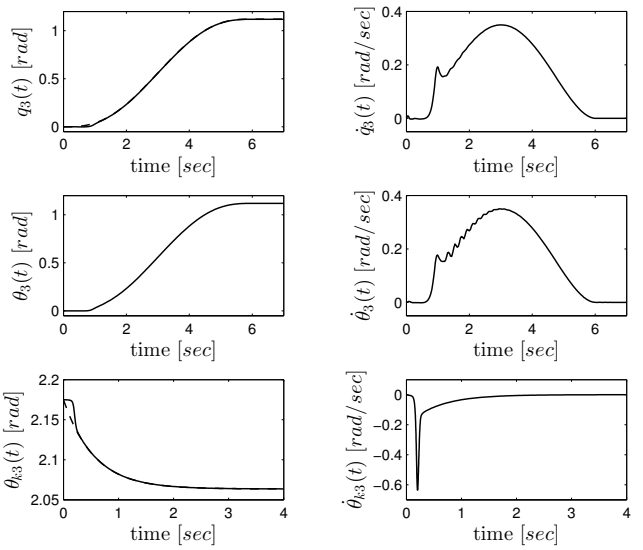

Fig. 6. Time evolution of the link, motor angles and velocities for the third joint alongside their references (dashed lines).

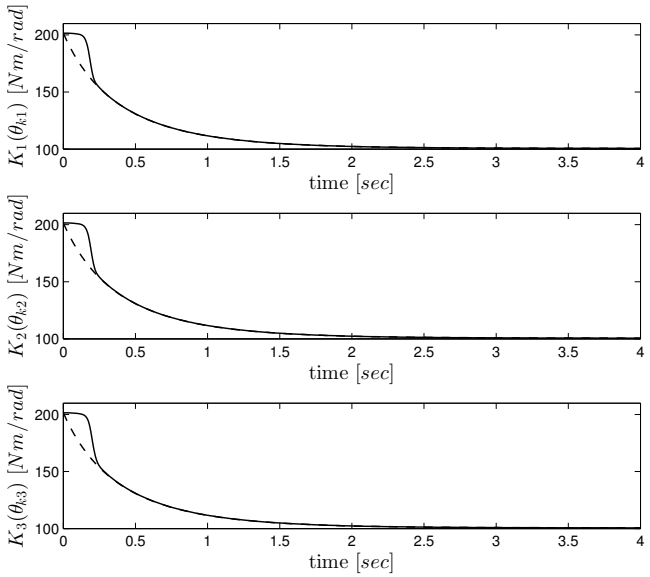

Fig. 7. Time evolution of the joints stiffness.

ideal motor transmissions with negligible internal losses. To investigate the robustness of the proposed control scheme with respect to the utilization of non ideal transmissions, losses are introduced in the motors' transmissions during the simulation. Specifically, it is assumed 30% loss in the transmission of the stiffness's motor of the second joint at $t = 2.5$ sec which increases to 40% loss at $t = 6$ sec. Furthermore, at $t = 5$ sec, 40% loss is introduced in the transmission of the link's motor of the first joint and 30% loss in the transmission of the link's motor of the third joint. Fig. 10 illustrates the demanded control efforts, where it is clear that the motors fast compensate (see subplots in Fig. 10) for the transmission losses. This disturbance however, is not reflected in the actual system outputs q_i, θ_{ki}, $i = 1, 2, 3$ which remain practically unaltered, and is as pictured in Figs. 4-6.

B. Comparison studies

In this subsection comparative studies are presented, in terms of tracking performance and robustness to external perturbations, with a gain scheduling controller that was recently reported in [15], to control single link variable stiffness actuated robots of the class considered in this work.

To model the variable stiffness actuator in our simulation study, we have employed the AwAS model [15] which is described by (2), (3) with joint stiffness $K(\theta_k)$ and reaction torque $F(\theta, q, \theta_k)$ given by:

$$\begin{aligned} K(\theta_k) &= K_{E2}(r_o - n_2\theta_k)^2, \\ F(\theta, q, \theta_k) &= -K_{R2}(r_o - n_2, \theta_k)(\theta - q)^2 \end{aligned}$$

where $K_{E2} = 160000\ N/m$, $K_{R2} = 63.662\ N/rad$, $r_o = 0.1$

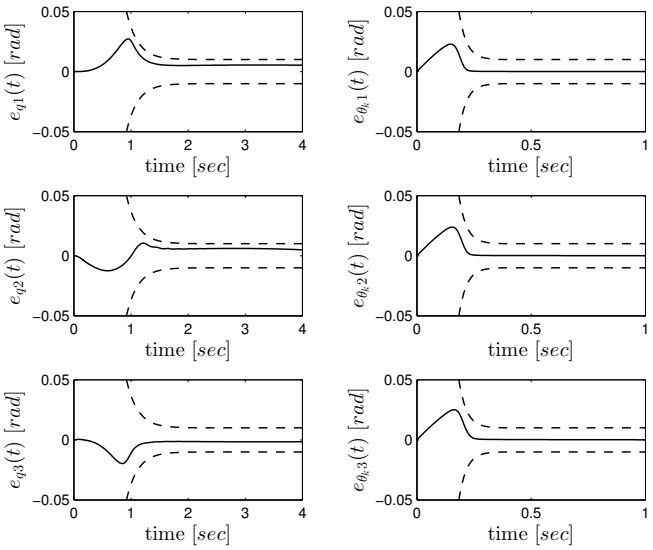

Fig. 8. Output errors (solid lines) with respect to performance envelopes (dashed lines).

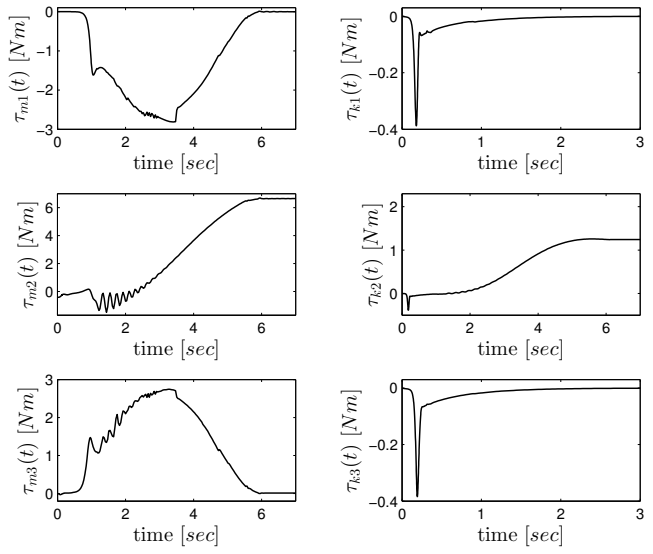

Fig. 9. The requested control efforts in case of ideal motor transmissions.

m, $n_2 = 3.98\times10^{-4}$ m/rad are construction specific mechanical constants. Also, $J_\theta = 0.0575$ kgm^2, $J_k = 6.8294\times10^{-5}$ kgm^2, $B_\theta = 10.2763$ Nms/rad, $B_k = 0.014$ Nms/rad, $K_\theta = 1.4139$ Nm/V and $K_k = 0.0227$ Nm/V.

According to [15], the original non-linear system was firstly approximated by a parametrized, in terms of the actuator stiffness, linear system, essentially constituting a set of linear time-invariant (LTI) systems. Subsequently, linear quadratic regulators (LQR) were designed for the LTIs and ultimately the gains of the LQRs undergo a polynomial fitting producing a gain scheduling controller. For the stiffness actuator, a PID controller was used. Following [15] PID gains are tuned for the linear part of the stiffness actuator model (equation (3) setting $F(\theta, q, \theta_k) = 0$). Speed of response for the stiffness actuator is shown to be faster than that of the link in [15]. Thus, in our case, we have found that for a constant stiffness

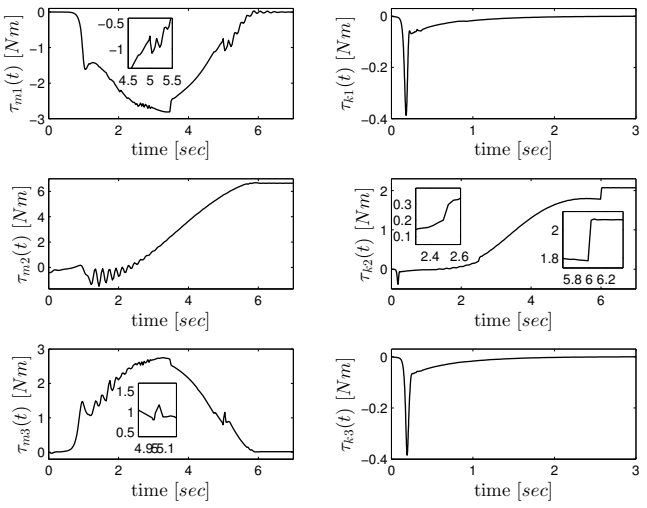

Fig. 10. The requested control efforts in case of losses in the transmissions.

in the range of [100, 1260] Nm/rad, the link's settling time ranges approximately from 0.4 sec for 100 Nm/rad to 0.09 sec for 1260 Nm/rad. Hence, the faster response of the stiffness actuator is fulfilled for all stiffness values by requiring 0.05 sec settling time. Furthermore, the overshoot is specified less than 15% and the disturbance rejection less than -40 dB at frequencies less than 25 rad/sec. These requirements lead to PID gains $K_P = 202, K_I = 808, K_D = 0.3$.

For the prescribed performance controller, it is required a steady state of no more than 0.01rad for the output errors $e_q(t)$ and $e_{\theta_k}(t)$ and minimum speed of convergence as obtained by the exponential e^{-8t} and e^{-9t} respectively. The aforementioned transient and steady state error bounds are prescribed by setting the parameters M_{ji} appearing in Theorem 1 to unity and using exponential performance functions as defined in (16) (see Appendix A). The remaining parameters are provided in Table III. Furthermore, the output and state error transformations were chosen as in (19). The closed loop system was simulated using control design constants given in Table IV, determined by following the procedure discussed in the 3-dof case.

TABLE III
PRESCRIBED PERFORMANCE FUNCTION PARAMETERS FOR THE ONE JOINT CASE

	ρ_0	ρ_∞	l
e_q	5	0.01	8
e_{v_q}	5.8	5.2	11.8
e_θ	2.2	0.25	8.2
e_{v_θ}	6	3.5	14.4
e_{θ_κ}	1	0.01	30
e_{v_κ}	2.3	0.4	11.5

Tracking performance: In the first set of comparisons, our purpose is to force the outputs q, θ_k to track the smooth, bounded trajectories $q_d(t) = 0.19 + 0.19\sin(3\pi t - \pi/2)$ and $\theta_{kd}(t) = 251.33 - 6.28\sqrt{K_d(t)}$, where $K_d(t) = 680 + 580\sin(0.2\pi t + \pi/3)$ is a desired stiffness trajectory ranging between the values of 99.85 and 1260 Nm/rad.

Notice that actuator stiffness is not available for measure-

TABLE IV
CONTROL DESIGN CONSTANTS FOR THE ONE JOINT CASE

j	κ_j	α_j
q	10.6	0.05
v_q	0.11	0.75
θ	3.3	4.5
v_θ	13.3	2
θ_κ	15	0.35
v_κ	0.2	2

ment and in that respect it is not incorporated in the control design. However, to guarantee fair comparison, the reference trajectory for the stiffness motor is produced by inverting the elastic torque model given in [15], for a desired joint stiffness trajectory, following current state of the art practices. In reality, actual joint stiffness may have diversions from the desired stiffness trajectory owing to modeling imperfections.

We set $\left[q(0)\ \dot{q}(0)\ \theta(0)\ \dot{\theta}(0)\ \theta_k(0)\ \dot{\theta}_k(0)\right]^\mathsf{T} = [0\ 0\ 0\ 0\ 35.28\ 0]^\mathsf{T}\ rad$. The initial value of θ_k corresponds to a stiffness value of $1182.3\ \mathrm{Nm/rad}$.

Fig. 11(a) depicts the link position error using the proposed prescribed performance controller and the one reported in [15]. It is clear that the prescribed performance controller guarantees the preselected output error despite the change of the stiffness value (Fig. 11(b)). The maximum error reported for the proposed prescribed performance controller is $\approx 0.2^o$ (0.003525 rad). However, for the controller [15] the same quantity appears significantly higher ($\approx 8^o$ (0.1379 rad)). The corresponding displacement for a link length 0.5 m yields 0.18 cm and 6.89 cm for the prescribed performance controller and the controller [15] respectively. For both cases, all the remaining closed loop signals are practically identical (e.g. the control efforts shown in Fig. 12) and thus are not presented in this study.

Robustness to external perturbations: We will now investigate the robustness of the two controllers to an external disturbance on the link. The disturbance $d(t)$ is introduced as three pulses of increasing magnitude and duration of 2 sec each, as shown in Fig. 13. Our purpose is to force the output q to track the smooth, bounded trajectory $q_d(t) = 0.0975 + 0.0975\tanh(10(t-0.8))$ while the actuator stiffness is kept at $100\ Nm/rad$, which represents a low stiffness value.

Fig. 14 shows the link position error and the control input for both the proposed prescribed performance controller (red line) and the controller presented in [15] (black line), when the disturbance is present (solid line) as well as absent (dashed line). The detail in Fig. 14 shows the output error for the prescribed performance controller in the presence of external disturbances (solid line) as well as without them (dashed line). The robustness of the prescribed performance controller is apparent since the output error continues to comply to the prescribed performance specifications despite the external disturbance, whereas in the case of controller [15] the presence of the disturbance is clearly reflected in the output error. Interestingly, both behaviours are achieved while demanding almost identical control efforts.

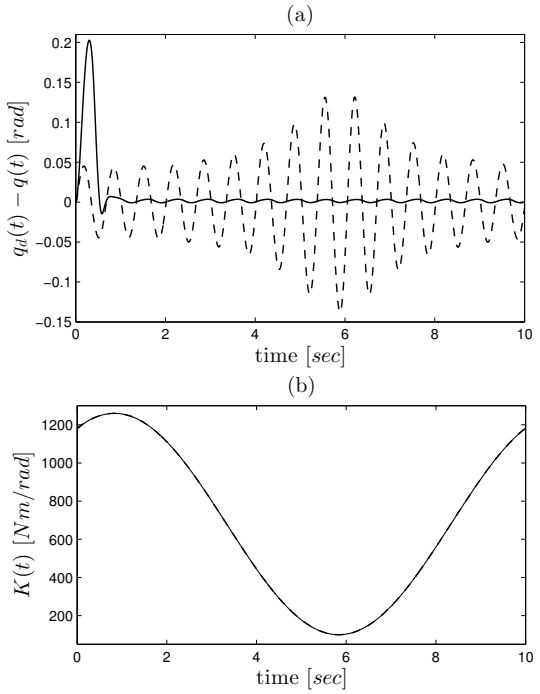

Fig. 11. (a) Link position error with the proposed controller (solid line) and the controller [15] (dashed line), (b) Evolution of the joint stiffness.

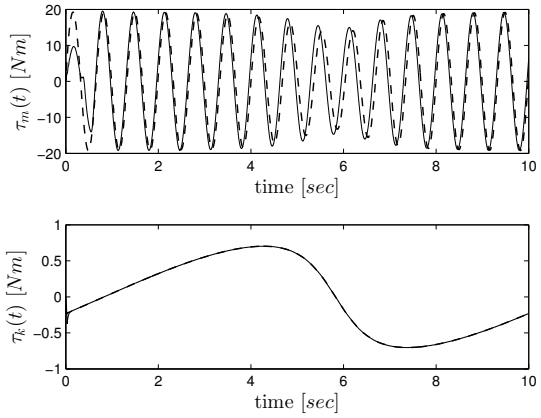

Fig. 12. The requested control effort with the proposed controller (solid line) and the controller [15] (dashed line).

V. CONCLUSION

A low complexity state feedback controller for variable stiffness actuated robots is presented achieving prescribed performance of the joint tracking and increased robustness to external perturbation outperforming the current state of the art control approaches particularly in low stiffness values. Extensive simulation studies incorporating actual VSA models highlight the aforementioned control attributes.

APPENDIX A
PRESCRIBED PERFORMANCE PRELIMINARIES

It will be clearly demonstrated in Appendix B that the control design is based on the prescribed performance control (PPC) methodology, which was pioneered in [28] and

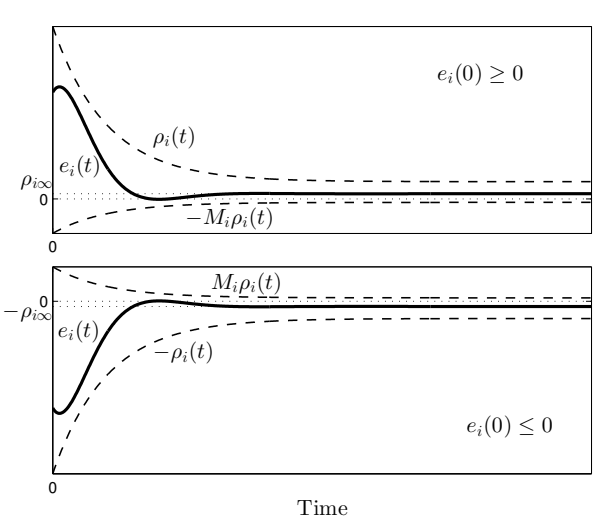

(a) Prescribed performance.

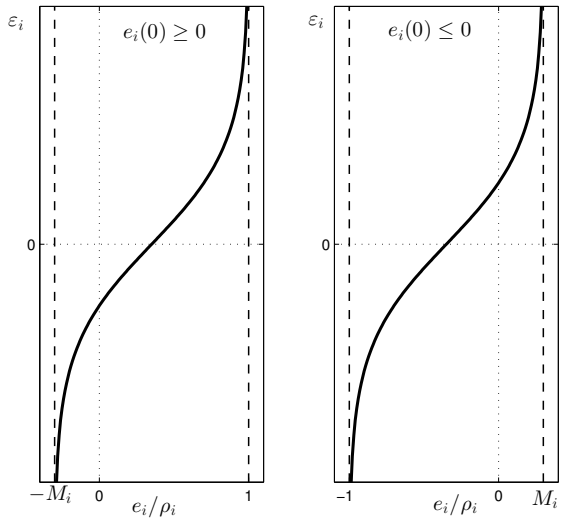

(b) The transformation function.

Fig. 15. Illustration of Prescribed Performance and Transformation Function.

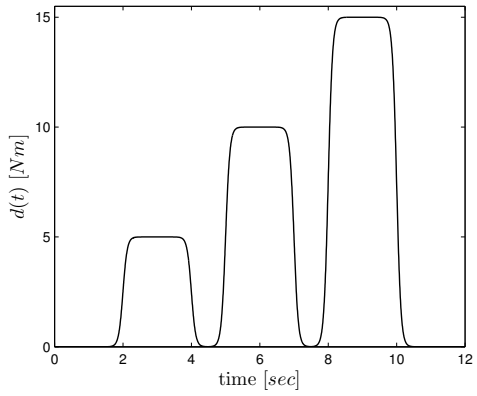

Fig. 13. External disturbance to the link.

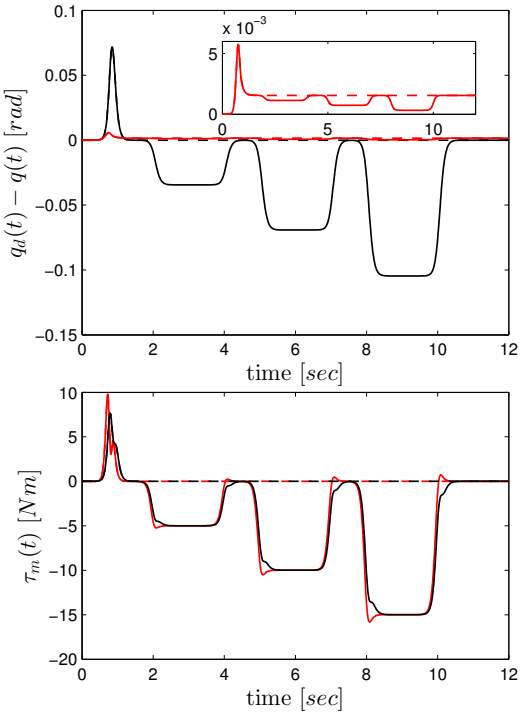

Fig. 14. Output error and control input for the prescribed performance controller (red line) and the controller [15] (black line). The dashed line corresponds to system response in the absence of external disturbance, while the solid line is the system response in the presence of external disturbances. The detail shows the output error for the prescribed performance controller.

utilized in [29]–[31] to design controllers capable of a priori guaranteeing prescribed performance bounds on the transient and steady state output error for a range of nonlinear system classes. Seeking a complete and self contained presentation, Appendix A summarizes preliminary knowledge on the concept of prescribed performance.

In that respect, consider a generic tracking error $e(t) = \left[\ e_1(t) \quad \ldots \quad e_m(t)\ \right]^{\mathsf{T}} \in \mathbb{R}^m$. Prescribed performance is achieved if each element $e_i(t)$, $i = 1, \ldots, m$ evolves strictly within a predefined region that is bounded by a decaying function of time. The mathematical expression of prescribed performance is given, $\forall t \geq 0$, by the following inequalities:

$$\left.\begin{array}{ll} -M_i\rho_i(t) < e_i(t) < \rho_i(t), & e_i(0) \geq 0 \\ -\rho_i(t) < e_i(t) < M_i\rho_i(t), & e_i(0) \leq 0 \end{array}\right\} \tag{15}$$

$i = 1, \ldots, m$, where $0 \leq M_i \leq 1$, $i = 1, \ldots, m$ and $\rho_i : \mathbb{R}_{\geq 0} \to \mathbb{R}_{>0}$, $i = 1, \ldots, m$ is a function of time that is bounded away from zero by a constant $c > 0$ and has a piecewise continuous and bounded derivative called performance function [28]. As (15) implies, only one set of the performance bounds is employed and specifically the one associated with the sign of $e_i(0)$. The aforementioned statements are clearly illustrated in Fig. 15a, for an exponential performance function

$$\rho_i(t) = (\rho_{i0} - \rho_{i\infty}) \exp(-l_i t) + \rho_{i\infty},\ i = 1, \ldots, m, \tag{16}$$

with ρ_{i0}, $\rho_{i\infty}$, l_i, $i = 1, \ldots, m$ strictly positive constants. The

constant $\rho_{i0} = \rho_i(0),\ i = 1, \ldots, m$ is selected such that (15) is satisfied at $t = 0$ (i.e., $\rho_i(0) > e_i(0)$ in case $e_i(0) \geq 0$ or $\rho_i(0) > -e_i(0)$ in case $e_i(0) \leq 0$). The constant $\rho_{i\infty} = \lim_{t\to\infty} \rho_i(t),\ i = 1, \ldots, m$ represents the maximum allowable size of $e_i(t)$ at the steady state that can be set arbitrarily small to a value reflecting the resolution of the measurement device, thus achieving practical convergence of $e_i(t)$ to zero. Furthermore, the decreasing rate of $\rho_i(t),\ i = 1, \ldots, m$, which is related to the constant $l_i,\ i = 1, \ldots, m$ in this case, introduces a lower bound on the required speed of convergence of $e_i(t)$. Moreover, the maximum overshoot is prescribed less than $M_i\rho_i(0),\ i = 1, \ldots, m$, which may even become zero by setting $M_i = 0,\ i = 1, \ldots, m$. Thus, the appropriate selection of the performance function $\rho_i(t),\ i = 1, \ldots, m$, as well as of the constant $M_i,\ i = 1, \ldots, m$, imposes performance bounds for the tracking error $e_i(t),\ i = 1, \ldots, m$.

To introduce prescribed performance, an error transformation is incorporated modulating the tracking error element $e_i(t),\ i = 1, \ldots, m$ with respect to the required performance bounds imposed by $\rho_i(t)$, $M_i,\ i = 1, \ldots, m$. More specifically, we define:

$$\varepsilon_i(t) = T_i\left(\frac{e_i(t)}{\rho_i(t)}\right),\ i = 1, \ldots, m \tag{17}$$

where $\varepsilon_i(t),\ i = 1, \ldots, m$ is the transformed error and $T_i(\cdot),\ i = 1, \ldots, m$ is a C^2 strictly increasing function defining a bijective mapping:

$$\left.\begin{array}{ll} T_i : (-M_i, 1) \to (-\infty, \infty), & e_i(0) \geq 0 \\ T_i : (-1, M_i) \to (-\infty, \infty), & e_i(0) \leq 0 \end{array}\right\} \tag{18}$$

$i = 1, \ldots, m$. A candidate transformation function, illustrated in Fig 15b, could be

$$T_i\left(\frac{e_i(t)}{\rho_i(t)}\right) = \begin{cases} a_i \ln\left(\frac{M_i + \frac{e_i(t)}{\rho_i(t)}}{1 - \frac{e_i(t)}{\rho_i(t)}}\right), & \text{in case } e_i(0) \geq 0 \\ a_i \ln\left(\frac{1 + \frac{e_i(t)}{\rho_i(t)}}{M_i - \frac{e_i(t)}{\rho_i(t)}}\right), & \text{in case } e_i(0) \leq 0 \end{cases} \tag{19}$$

$i = 1, \ldots, m$, where a_i are positive design constants. As (18) implies and the aforementioned example clarifies, the choice of the mapping $T_i(\cdot),\ i = 1, \ldots, m$, depends only on the sign of $e_i(0),\ i = 1, \ldots, m$. Notice also that since $\rho_i(0),\ i = 1, \ldots, m$ is selected such that (15) is satisfied at $t = 0$, $\varepsilon_i(0),\ i = 1, \ldots, m$ is finite owing to (18). Furthermore, the case of $e_i(0) = 0$ requires selection of $M_i \neq 0,\ i = 1, \ldots, m$, since otherwise (i.e., $M_i = 0$) $\varepsilon_i(0),\ i = 1, \ldots, m$ becomes infinite.

Owing to the properties of the error transformation, prescribed performance in the sense of (15) is satisfied by keeping $\varepsilon_i(t),\ i = 1, \ldots, m$ bounded. Notice that the bounds of $\varepsilon_i(t),\ i = 1, \ldots, m$ do not affect the evolution of $e_i(t),\ i = 1, \ldots, m$, which are solely prescribed by (15) and thus by the selection of the performance functions $\rho_i(t),\ i = 1, \ldots, m$ as well as the constants $M_i,\ i = 1, \ldots, m$.

APPENDIX B
PROOF OF THEOREM 1

We initially formulate the closed loop system dynamics in the transformed error space. Employing the definitions of the output and state errors $e_q, e_{\theta_k}, e_{v_q}, e_\theta, e_{v_\theta}, e_{v_k}$, it is obtained

$$e_j = \left[\rho_{j1}T_{j1}^{-1}(\varepsilon_{j1})\ \ \ldots\ \ \rho_{jn}T_{jn}^{-1}(\varepsilon_{jn})\right]^{\mathsf{T}}, \tag{20}$$

$j \in \{q, \theta_k, v_q, \theta, v_\theta, v_k\}$. For compactness of presentation we shall denote $\rho_j T_j^{-1}(\varepsilon_j) \triangleq e_j$, $j \in \{q, \theta_k, v_q, \theta, v_\theta, v_k\}$. Hence, employing (9)-(14), it is straightforwardly obtained:

$$\begin{aligned} q &= q_d(t) + e_q && (21)\\ &= q_d(t) + \rho_q T_q^{-1}(\varepsilon_q) && (22)\\ \dot{q} &= v_q(t) + e_{v_q} && (23)\\ &= -\kappa_q(\Psi_q + \Psi_q^{-1})\varepsilon_q + \rho_{v_q}T_{v_q}^{-1}(\varepsilon_{v_q}) && (24)\\ \theta &= \theta_r(t) + e_\theta && (25)\\ &= -\kappa_{v_q}\Psi_{v_q}\varepsilon_{v_q} + \rho_\theta T_\theta^{-1}(\varepsilon_\theta) && (26)\\ \dot{\theta} &= v_\theta(t) + e_{v_\theta} && (27)\\ &= -\kappa_\theta(\Psi_\theta + \Psi_\theta^{-1})\varepsilon_\theta + \rho_{v_\theta}T_{v_\theta}^{-1}(\varepsilon_{v_\theta}) && (28)\\ \theta_k &= \theta_{kd}(t) + e_{\theta_k} && (29)\\ &= \theta_{kd}(t) + \rho_{\theta_k}T_{\theta_k}^{-1}(\varepsilon_{\theta_k}) && (30)\\ \dot{\theta}_k &= v_{\theta_k}(t) + e_{v_k} && (31)\\ &= -\kappa_{\theta_k}(\Psi_{\theta_k} + \Psi_{\theta_k}^{-1})\varepsilon_{\theta_k} + \rho_{v_k}T_{v_k}^{-1}(\varepsilon_{v_k}). && (32) \end{aligned}$$

The link and motor accelerations with respect to the transformed errors are derived as

$$\begin{aligned} \ddot{q} &= -\mathcal{Z}_q(\varepsilon_q, \varepsilon_{v_q}, t) - \mathcal{Z}_{E_q}(\varepsilon_q, \varepsilon_{\theta_k}, t)(q - \theta) && (33)\\ \ddot{\theta} &= -\mathcal{Z}_\theta(\varepsilon_\theta, \varepsilon_{v_\theta}, t) - \mathcal{Z}_{E_\theta}(\varepsilon_{\theta_k}, \varepsilon_\theta, \varepsilon_q, \varepsilon_{v_q}, t) \\ &\qquad + J_\theta^{-1}K_\theta u_m && (34)\\ \ddot{\theta}_k &= -\mathcal{Z}_{\theta_k}(\varepsilon_{\theta_k}, \varepsilon_{v_k}, t) - \mathcal{Z}_k(\varepsilon_{\theta_k}, \varepsilon_\theta, \varepsilon_q, \varepsilon_{v_q}, t) \\ &\qquad + J_k^{-1}K_k u_k && (35) \end{aligned}$$

where

$$\begin{aligned} \mathcal{Z}_q(\varepsilon_q, \varepsilon_{v_q}, t) &= M^{-1}(q)\left[C(q, \dot{q})\dot{q} + G(q)\right] && (36)\\ \mathcal{Z}_{E_q}(\varepsilon_q, \varepsilon_{\theta_k}, t) &= M^{-1}(q)K(\theta_k) && (37)\\ \mathcal{Z}_\theta(\varepsilon_\theta, \varepsilon_{v_\theta}, t) &= J_\theta^{-1}B_\theta\dot{\theta} && (38)\\ \mathcal{Z}_{E_\theta}(\varepsilon_{\theta_k}, \varepsilon_\theta, \varepsilon_q, \varepsilon_{v_q}, t) &= J_\theta^{-1}K(\theta_k)(\theta - q) && (39)\\ \mathcal{Z}_{\theta_k}(\varepsilon_{\theta_k}, \varepsilon_{v_k}, t) &= J_k^{-1}B_k\dot{\theta}_k && (40)\\ \mathcal{Z}_k(\varepsilon_{\theta_k}, \varepsilon_\theta, \varepsilon_q, \varepsilon_{v_q}, t) &= F(\theta, q, \theta_k) && (41) \end{aligned}$$

In the aforementioned expression, the variables $q, \dot{q}, \theta, \dot{\theta}, \theta_k, \dot{\theta}_k$ are related to ε_j, $j \in \{q, \theta_k, v_q, \theta, v_\theta, v_k\}$ and t via (22), (24), (26), (28), (30), (32).

Differentiating (7) with respect to time and using (8), we obtain:

$$\begin{aligned} \dot{\varepsilon}_j &= \begin{bmatrix} \frac{1}{\rho_{j1}}\frac{\partial T_{j1}}{\partial\left(\frac{e_{j1}}{\rho_{j1}}\right)}\left(\dot{e}_{j1} - e_{j1}\frac{\dot{\rho}_{j1}}{\rho_{j1}}\right) \\ \vdots \\ \frac{1}{\rho_{jn}}\frac{\partial T_{jn}}{\partial\left(\frac{e_{jn}}{\rho_{jn}}\right)}\left(\dot{e}_{jn} - e_{jn}\frac{\dot{\rho}_{jn}}{\rho_{jn}}\right) \end{bmatrix} \\ &= \Psi_j\ (\dot{e}_j - \nu_j(\varepsilon_j, t)),\ j \in \{q, \theta_k, v_q, \theta, v_\theta, v_k\} \end{aligned} \tag{42}$$

where $\nu_j(\varepsilon_j, t)$ is defined using (20) as follows:

$$\begin{aligned} \nu_j(\varepsilon_j, t) &= \begin{bmatrix} e_{j1}\frac{\dot{\rho}_{j1}}{\rho_{j1}} & \ldots & e_{jn}\frac{\dot{\rho}_{jn}}{\rho_{jn}} \end{bmatrix}^{\mathsf{T}} \\ &= \left[\dot{\rho}_{j1}(t)T_{j1}^{-1}(\varepsilon_{j1})\ \ \ldots\ \ \dot{\rho}_{jn}(t)T_{jn}^{-1}(\varepsilon_{jn})\right]^{\mathsf{T}}, \end{aligned}$$

with $j \in \{q, \theta_k, v_q, \theta, v_\theta, v_k\}$. Substituting (20), (21), (23), (25), (27), (29), (31) in (42) using the error definitions yields:

$$\begin{aligned}
\dot{\varepsilon}_q &= \Psi_q\ (\dot{e}_q - \nu_q(\varepsilon_q, t)) \\
&= \Psi_q\ (\dot{q} - \dot{q}_d(t) - \nu_q(\varepsilon_q, t)) \\
&= \Psi_q\ (v_q(t) + \rho_{v_q} T_{v_q}^{-1}(\varepsilon_{v_q}) - \dot{q}_d(t) - \nu_q(\varepsilon_q, t)) \\
\dot{\varepsilon}_{\theta_k} &= \Psi_{\theta_k}\ (\dot{e}_{\theta_k} - \nu_{\theta_k}(\varepsilon_{\theta_k}, t)) \\
&= \Psi_{\theta_k}\ (\dot{\theta}_k - \dot{\theta}_{kd}(t) - \nu_{\theta_k}(\varepsilon_{\theta_k}, t)) \\
&= \Psi_{\theta_k}\ (v_{\theta_k}(t) + \rho_{v_k} T_{v_k}^{-1}(\varepsilon_{v_k}) - \dot{\theta}_{kd}(t) - \nu_{\theta_k}(\varepsilon_{\theta_k}, t)) \\
\dot{\varepsilon}_{v_q} &= \Psi_{v_q}\ (\dot{e}_{v_q} - \nu_{v_q}(\varepsilon_{v_q}, t)) \\
&= \Psi_{v_q}\ (\ddot{q} - \dot{v}_q(t) - \nu_{v_q}(\varepsilon_{v_q}, t)) \\
\dot{\varepsilon}_\theta &= \Psi_\theta\ (\dot{e}_\theta - \nu_\theta(\varepsilon_\theta, t)) \\
&= \Psi_\theta\ (\dot{\theta} - \dot{\theta}_r(t) - \nu_\theta(\varepsilon_\theta, t)) \\
&= \Psi_\theta\ (v_\theta(t) + \rho_{v_\theta} T_{v_\theta}^{-1}(\varepsilon_{v_\theta}) - \dot{\theta}_r(t) - \nu_\theta(\varepsilon_{v_\theta}, t)) \\
\dot{\varepsilon}_{v_\theta} &= \Psi_{v_\theta}\ (\dot{e}_{v_\theta} - \nu_{v_\theta}(\varepsilon_{v_\theta}, t)) \\
&= \Psi_{v_\theta}\ (\ddot{\theta} - \dot{v}_\theta(t) - \nu_{v_\theta}(\varepsilon_{v_\theta}, t)) \\
\dot{\varepsilon}_{v_k} &= \Psi_{v_k}\ (\dot{e}_{v_k} - \nu_{v_k}(\varepsilon_{v_k}, t)) \\
&= \Psi_{v_k}\ (\ddot{\theta}_k - \dot{v}_{\theta_k}(t) - \nu_{v_k}(\varepsilon_{v_k}, t))
\end{aligned}$$

Finally, substituting the controller (9) - (14) and the system dynamics (33) - (35) the closed loop dynamics in the transformed error space can be written as follows:

$$\begin{aligned}
\dot{\varepsilon}_q &= -\kappa_q \varepsilon_q - \kappa_q \Psi_q^2 \varepsilon_q - \Psi_q\left(\dot{q}_d(t) + \nu_q(\varepsilon_q, t)\right) \\
&\quad + \Psi_q \rho_{v_q} T_{v_q}^{-1}(\varepsilon_{v_q}) \qquad (43) \\
\dot{\varepsilon}_{\theta_k} &= -\kappa_{\theta_k} \varepsilon_{\theta_k} - \kappa_{\theta_k} \Psi_{\theta_k}^2 \varepsilon_{\theta_k} \\
&\quad - \Psi_{\theta_k}\left(\dot{\theta}_{kd}(t) + \nu_{\theta_k}(\varepsilon_{\theta_k}, t)\right) \\
&\quad + \Psi_{\theta_k} \rho_{v_k} T_{v_k}^{-1}(\varepsilon_{v_k}) \qquad (44) \\
\dot{\varepsilon}_{v_q} &= -\Psi_{v_q} \mathcal{Z}_{E_q}(\varepsilon_q, \varepsilon_{\theta_k}, t) \kappa_{v_q} \Psi_{v_q} \varepsilon_{v_q} \\
&\quad + \Psi_{v_q}\big\{-\mathcal{Z}_q(\varepsilon_q, \varepsilon_{v_q}, t) - \dot{v}_q - \nu_{v_q}(\varepsilon_{v_q}, t) - \\
&\qquad - \mathcal{Z}_{E_q}(\varepsilon_q, \varepsilon_{\theta_k}, t)\left(q_d + \rho_q T_q^{-1}(\varepsilon_q)\right. \\
&\qquad \left. - \rho_\theta T_\theta^{-1}(\varepsilon_\theta)\right)\big\} \qquad (45) \\
\dot{\varepsilon}_\theta &= -\kappa_\theta \varepsilon_\theta - \kappa_\theta \Psi_\theta^2 \varepsilon_\theta \\
&\quad - \Psi_\theta\left(\dot{\theta}_r(t) + \nu_\theta(\varepsilon_\theta, t)\right) + \Psi_\theta \rho_{v_\theta} T_{v_\theta}^{-1}(\varepsilon_{v_\theta}) \qquad (46) \\
\dot{\varepsilon}_{v_\theta} &= -J_\theta^{-1} K_\theta \kappa_{v_\theta}(\varepsilon_{v_\theta} + \Psi_{v_\theta}^2 \varepsilon_{v_\theta}) \\
&\quad + \Psi_{v_\theta}\big\{-\mathcal{Z}_\theta(\varepsilon_\theta, \varepsilon_{v_\theta}, t) \\
&\quad - \mathcal{Z}_{E_\theta}(\varepsilon_{\theta_k}, \varepsilon_\theta, \varepsilon_q, \varepsilon_{v_q}, t) - \dot{v}_\theta - \nu_{v_\theta}(\varepsilon_{v_\theta}, t)\big\} \qquad (47) \\
\dot{\varepsilon}_{v_k} &= -J_k^{-1} K_k \kappa_{v_k}(\varepsilon_{v_k} + \Psi_{v_k}^2 \varepsilon_{v_k}) \\
&\quad + \Psi_{v_k}\big\{-\mathcal{Z}_{\theta_k}(\varepsilon_{\theta_k}, \varepsilon_{v_\theta k}, t) \\
&\quad - \mathcal{Z}_k(\varepsilon_{\theta_k}, \varepsilon_\theta, \varepsilon_q, \varepsilon_{v_q}, t) - \dot{v}_{\theta_k} - \nu_{v_k}(\varepsilon_{v_k}, t)\big\} \qquad (48)
\end{aligned}$$

According to the prescribed performance preliminaries, the *PPC/VSA problem* is solved if the uniform boundedness of $\varepsilon_j,\ j = \{q, \theta_k, v_q, \theta, v_\theta, v_k\}$, is proved. The proof proceeds in a stepwise manner as follows.

Step 1 (ε_q, ε_{θ_k}-subsystems): At first we consider the ε_q, ε_{θ_k} subsystems (43), (44) and the positive definite and radially unbounded Lyapunov function candidate $V_1 = \frac{1}{2}\ \varepsilon_q^\mathsf{T} \varepsilon_q + \frac{1}{2}\ \varepsilon_{\theta_k}^\mathsf{T} \varepsilon_{\theta_k}$. The time derivative of V_1 along the solutions of (43), (44) yields

$$\begin{aligned}
\dot{V}_1 &= -\sum_{i \in \{q, \theta_k\}} \kappa_i \|\varepsilon_i\|^2 - \sum_{i \in \{q, \theta_k\}} \kappa_i \|\Psi_i \varepsilon_i\|^2 + \sum_{i \in \{q, \theta_k\}} \varepsilon_i^\mathsf{T} \Psi_i \mathcal{B}_i \\
&\leq -\sum_{i \in \{q, \theta_k\}} \kappa_i \|\varepsilon_i\|^2 - \sum_{i \in \{q, \theta_k\}} \kappa_i \|\Psi_i \varepsilon_i\|^2 \\
&\quad + \sum_{i \in \{q, \theta_k\}} \|\varepsilon_i^\mathsf{T} \Psi_i\| \|\mathcal{B}_i\|
\end{aligned}$$

where

$$\mathcal{B}_q = \left(\rho_{v_q} T_{v_q}^{-1}(\varepsilon_{v_q}) - \dot{q}_d(t) - \nu_q(\varepsilon_q, t)\right) \qquad (49)$$

$$\mathcal{B}_{\theta_k} = \left(\rho_{\theta_k} T_{v_k}^{-1}(\varepsilon_{v_k}) - \dot{\theta}_{kd}(t) - \nu_{\theta_k}(\varepsilon_{\theta_k}, t)\right) \qquad (50)$$

Completing the squares we finally arrive at

$$\dot{V}_1 \leq -\sum_{i \in \{q, \theta_k\}} \kappa_i \|\varepsilon_i\|^2 + \sum_{i \in \{q, \theta_k\}} \frac{1}{4\kappa_i} \|\mathcal{B}_i\|^2$$

To continue, notice that in (49), (50) $\rho_{v_q} T_{v_q}^{-1}(\varepsilon_{v_q}) \in \mathcal{L}_\infty$ and $\rho_{\theta_k} T_{v_k}^{-1}(\varepsilon_{v_k}) \in \mathcal{L}_\infty$ since $\rho_{v_q}(t)$, $\rho_{\theta_k}(t)$ are bounded functions of time by definition and $T_{v_q}^{-1}(\varepsilon_{v_q})$, $T_{v_k}^{-1}(\varepsilon_{v_k})$ are bounded by construction. Moreover,

$$\nu_q(\varepsilon_q, t) = \left[\dot{\rho}_{q1}(t) T_{q1}^{-1}(\varepsilon_{q1})\ \ \ldots\ \ \dot{\rho}_{qn}(t) T_{qn}^{-1}(\varepsilon_{qn})\right]^\mathsf{T},$$

$$\nu_{\theta_k}(\varepsilon_{\theta_k}, t) = \left[\dot{\rho}_{\theta_k 1}(t) T_{\theta_k 1}^{-1}(\varepsilon_{\theta_k 1})\ \ \ldots\ \ \dot{\rho}_{\theta_k n}(t) T_{\theta_k n}^{-1}(\varepsilon_{\theta_k n})\right]^\mathsf{T}.$$

Hence, $\nu_q(\varepsilon_q, t),\ \nu_{\theta_k}(\varepsilon_{\theta_k}, t) \in \mathcal{L}_\infty$ since $\dot{\rho}_q(t),\ \dot{\rho}_{\theta_k}(t)$ are bounded functions of time by definition and $T_q^{-1}(\varepsilon_q)$, $T_{\theta_k}^{-1}(\varepsilon_{\theta_k})$ are bounded by construction. Finally, $\dot{q}_d(t)$, $\dot{\theta}_{kd}(t)$ are bounded owing to the smoothness and boundedness of $q_d(t)$ and $\theta_{kd}(t)$. Therefore, the terms $\|\mathcal{B}_i\|^2,\ i \in \{q, \theta_k\}$ are also bounded and let $c_i = \sup_t \|\mathcal{B}_i\|^2 > 0,\ i \in \{q, \theta_k\}$. Thus, $\dot{V}_1$ becomes

$$\dot{V}_1 \leq -\sum_{i \in \{q, \theta_k\}} \kappa_i \|\varepsilon_i\|^2 + \sum_{i \in \{q, \theta_k\}} \frac{c_i}{4\kappa_i} \qquad (51)$$

From (51) we conclude the uniform ultimate boundedness of $\varepsilon_i\ i \in \{q, \theta_k\}$ with respect to the sets

$$\mathcal{E}_i = \left\{\|\varepsilon_i\| \in \mathbb{R} : \|\varepsilon_i\| \leq \frac{\sqrt{c_i}}{2\kappa_i}\right\},\ \ i \in \{q, \theta_k\}$$

and hence their uniform boundedness as well. Consequently $\Psi_i,\ i \in \{q, \theta_k\}$ are bounded, while $\Psi_i^{-1}(\varepsilon_i),\ i \in \{q, \theta_k\}$ as defined in (8) are bounded by construction. It is therefore straightforward to conclude from (43),(44) the boundedness of $\dot{\varepsilon}_i(t),\ i \in \{q, \theta_k\}$ which further implies the boundedness of $v_i,\ i \in \{q, \theta_k\}$ owing to (12), (14). Furthermore,

$$\dot{v}_i = -\kappa_i \left[(\vartheta \dot{T}_i + \vartheta \dot{T}_i^{-1})\varepsilon_i + (\Psi_i + \Psi_i^{-1})\dot{\varepsilon}_i\right] \in \mathcal{L}_\infty$$

,$i \in \{q, \theta_k\}$ since $\varepsilon_i, \dot{\varepsilon}_i, \Psi_i, \Psi_i^{-1},\ i \in \{q, \theta_k\}$ were already proved bounded and $\vartheta \dot{T}_i, \vartheta \dot{T}_i^{-1}, i \in \{q, \theta_k\}$ are bounded since Ψ_i, Ψ_i^{-1} are smooth and bounded.

Step 2 (ε_{v_q}-subsystem): Consider now (45) and the positive definite, radially unbounded Lyapunov function candidate

$V_2 = \frac{1}{2}\ \varepsilon_{v_q}^{\mathsf{T}}\varepsilon_{v_q}$. Following identical arguments as in Step 1, the time derivative of V_2 yields

$$\begin{aligned}\dot{V}_2 \ &\leq\ -\kappa_{v_q}\lambda_M K_M(\theta_k)\|\Psi_{v_q}\varepsilon_{v_q}\|^2 \\ &\quad -\kappa_{v_q}\varepsilon_{v_q}^{\mathsf{T}}\Psi_{v_q}M^{-1}(q)\Delta K(\theta_k)\Psi_{v_q}\varepsilon_{v_q} \\ &\quad +\|\varepsilon_{v_q}^{\mathsf{T}}\Psi_{v_q}\|\|\mathcal{B}_{v_q}\|\end{aligned}$$

where

$$\begin{aligned}\mathcal{B}_{v_q} \ &=\ -\mathcal{Z}_q(\varepsilon_q,\varepsilon_{v_q},t) - \dot{v}_q - \nu_{v_q}(\varepsilon_{v_q},t) - \\ &\quad -\mathcal{Z}_{E_q}(\varepsilon_q,\varepsilon_{\theta_k},t)\left(q_d + \rho_q T_q^{-1}(\varepsilon_q)\right. \\ &\quad \left.-\rho_\theta T_\theta^{-1}(\varepsilon_\theta)\right) \qquad (52)\end{aligned}$$

and we have used the well known property for the robot's inertia matrix $M(q)$, that there exist constants λ_m, λ_M satisfying $\lambda_M > \lambda_m > 0$ such that

$$\lambda_m\mathcal{I} \leq M(q) \leq \lambda_M\mathcal{I} \qquad (53)$$

Splitting the first term as follows:

$$\begin{aligned}-\kappa_{v_q}K_M(\theta_k)\lambda_M\|\Psi_{v_q}\varepsilon_{v_q}\|^2 = \\ -\frac{1}{\gamma}\kappa_{v_q}K_M(\theta_k)\lambda_M\|\Psi_{v_q}\varepsilon_{v_q}\|^2 \\ -\frac{\gamma-1}{2\gamma}\kappa_{v_q}K_M(\theta_k)\lambda_M\|\Psi_{v_q}\varepsilon_{v_q}\|^2 \\ -\frac{\gamma-1}{2\gamma}\kappa_{v_q}K_M(\theta_k)\lambda_M\|\Psi_{v_q}\varepsilon_{v_q}\|^2\end{aligned}$$

with $\gamma > 1$ a constant. Utilising (53) we obtain

$$\begin{aligned}\dot{V}_2 \ &\leq\ -\frac{1}{\gamma}\kappa_{v_q}K_M(\theta_k)\lambda_M\|\Psi_{v_q}\varepsilon_{v_q}\|^2 \\ &\quad -\frac{\gamma-1}{2\gamma}\kappa_{v_q}K_M(\theta_k)\lambda_M\|\Psi_{v_q}\varepsilon_{v_q}\|^2 \\ &\quad -\frac{\gamma-1}{2\gamma}\kappa_{v_q}K_M(\theta_k)\lambda_M\|\Psi_{v_q}\varepsilon_{v_q}\|^2 \\ &\quad +\kappa_{v_q}\lambda_m\lambda_{\Delta K}\|\Psi_{v_q}\varepsilon_{v_q}\|^2 + \|\varepsilon_{v_q}^{\mathsf{T}}\Psi_{v_q}\|\|\mathcal{B}_{v_q}\|\end{aligned}$$

where

$$\begin{aligned}\lambda_{\Delta K}(\theta_k) \ &=\ \max_i\{|K_i(\theta_{k_i}) - K_M(\theta_k)|\} \\ &=\ K_M(\theta_k) - \min_i\{K_i(\theta_{k_i})\} > 0, \qquad (54)\end{aligned}$$

$\forall\theta_k > 0$, with $K_i(\theta_{k_i})$, $i = 1,\ldots,n$ the elements of the $K(\theta_k)$ matrix. Completing the squares we obtain

$$\begin{aligned}&-\frac{\gamma-1}{2\gamma}\kappa_{v_q}K_M(\theta_k)\lambda_M\|\Psi_{v_q}\varepsilon_{v_q}\|^2 + \|\varepsilon_{v_q}^{\mathsf{T}}\Psi_{v_q}\|\|\mathcal{B}_{v_q}\| \\ \leq\ &\frac{\gamma}{2(\gamma-1)\kappa_{v_q}K_M(\theta_k)\lambda_M}\|\mathcal{B}_{v_q}\|^2\end{aligned}$$

Hence $\dot{V}_2$ becomes

$$\begin{aligned}\dot{V}_2 \ \leq\ &-\frac{1}{\gamma}\kappa_{v_q}K_M(\theta_k)\lambda_M\|\Psi_{v_q}\varepsilon_{v_q}\|^2 \\ &-\frac{\gamma-1}{2\gamma}\kappa_{v_q}K_M(\theta_k)\lambda_M\|\Psi_{v_q}\varepsilon_{v_q}\|^2 \\ &+\frac{\gamma\|\mathcal{B}_{v_q}\|^2}{2(\gamma-1)\kappa_{v_q}K_M(\theta_k)\lambda_M} + \kappa_{v_q}\lambda_m\lambda_{\Delta K}\|\Psi_{v_q}\varepsilon_{v_q}\|^2.\end{aligned}$$

Claim 1 There exists a $\gamma > 1$ such that the following inequality holds:

$$\frac{\lambda_{\Delta K}(\theta_k)}{K_M(\theta_k)} \leq \frac{1}{\gamma}\frac{\lambda_M}{\lambda_m}, \quad \forall\theta_k > 0. \qquad (55)$$

Proof. From (6), (54), notice that $\forall\theta_k > 0$

$$\begin{aligned}\frac{\lambda_{\Delta K}(\theta_k)}{K_M(\theta_k)} \ &=\ \frac{\max_i\{K_i(\theta_{k_i})\} - \min_i\{K_i(\theta_{k_i})\}}{\max_i\{K_i(\theta_{k_i})\}} \\ &=\ 1 - \frac{\min_i\{K_i(\theta_{k_i})\}}{\max_i\{K_i(\theta_{k_i})\}} \\ &<\ 1.\end{aligned}$$

Therefore, since $\frac{\lambda_M}{\lambda_m} > 1$, we conclude that there exists a positive constant $\gamma > 1$, such that (55) holds.

■

Using Claim 1, we straightforwardly conclude that

$$-\frac{1}{\gamma}\kappa_{v_q}K_M(\theta_k)\lambda_M\|\Psi_{v_q}\varepsilon_{v_q}\|^2 + \kappa_{v_q}\lambda_m\lambda_{\Delta K}\|\Psi_{v_q}\varepsilon_{v_q}\|^2 \leq 0.$$

Therefore, $\dot{V}_2$ finally becomes

$$\begin{aligned}\dot{V}_2 \ \leq\ &-\frac{\gamma-1}{2\gamma}\kappa_{v_q}K_M(\theta_k)\lambda_M\|\Psi_{v_q}\varepsilon_{v_q}\|^2 \\ &+\frac{\gamma}{2(\gamma-1)\kappa_{v_q}K_M(\theta_k)\lambda_M}\|\mathcal{B}_{v_q}\|^2. \qquad (56)\end{aligned}$$

To proceed we need to show the boundedness of $\|\mathcal{B}_{v_q}\|$ defined in (52). In Step 1 we have proved the boundedness of $\varepsilon_q, \varepsilon_{\theta_k}$. Moreover, q_d and θ_{kd} are bounded by definition. To continue, $\rho_\theta T_\theta^{-1}(\varepsilon_\theta) \in \mathcal{L}_\infty$ and $\rho_q T_q^{-1}(\varepsilon_q) \in \mathcal{L}_\infty$ since ρ_θ and ρ_q are smooth and bounded functions of time by definition and $T_\theta^{-1}(\varepsilon_\theta)$, $T_q^{-1}(\varepsilon_q)$ are bounded by construction. Furthermore $\dot{v}_q$ was proven bounded in Step 1 and

$$\nu_{v_q}(\varepsilon_{v_q},t) = \left[\dot{\rho}_{v_q1}(t)T_{v_q1}^{-1}(\varepsilon_{v_q1})\ \ldots\ \dot{\rho}_{v_qn}(t)T_{v_qn}^{-1}(\varepsilon_{v_qn})\right]^{\mathsf{T}}$$

is bounded by construction. Additionally, owing to (4) and (22), (24), (30), (36), (37) the terms $\mathcal{Z}_q(\varepsilon_q,\varepsilon_{v_q},t)$ and $\mathcal{Z}_{E_q}(\varepsilon_q,\varepsilon_{\theta_k},t)$ are also bounded. Therefore, all terms appearing in (52) are bounded, which directly leads to the boundedness of $\|\mathcal{B}_{v_q}\|$. If we denote by $c_{v_q} = \sup_t\|\mathcal{B}_{v_q}\|^2 > 0$, $\dot{V}_2$ becomes:

$$\begin{aligned}\dot{V}_2 \ \leq\ &-\frac{\gamma-1}{2\gamma}\kappa_{v_q}K_M(\theta_k)\lambda_M\|\Psi_{v_q}\varepsilon_{v_q}\|^2 \qquad (57) \\ &+\frac{\gamma c_{v_q}}{2(\gamma-1)\kappa_{v_q}K_M(\theta_k)\lambda_M} \qquad (58)\end{aligned}$$

From (57) we conclude the uniform ultimate boundedness of $\|\Psi_{v_q}\varepsilon_{v_q}\|$ with respect to the set $\mathcal{E}_{v_q} = \left\{\|\Psi_{v_q}\varepsilon_{v_q}\| \in \Re : \|\Psi_{v_q}\varepsilon_{v_q}\| \leq \frac{\gamma\sqrt{c_{v_q}}}{(\gamma-1)\kappa_{v_q}K_M(\theta_k)\lambda_M}\right\}$ and thus its uniform boundedness as well. Let $a_{v_q} > 0$ be an (unknown) upper bound. Since $\|\Psi_{v_q}\varepsilon_{v_q}\| \leq a_{v_q}$, we straightforwardly conclude that

$$|\Psi_{v_qi}\ \varepsilon_{v_qi}| = |\Psi_{v_qi}||\varepsilon_{v_qi}| \leq a_{v_q},\ \forall i = 1,\ldots,n. \qquad (59)$$

Moreover, by definition $0 < \rho_{v_qi}(t) < \rho_{v_q0i},\ \forall i = 1,2,\ldots,n$ and T_{v_qi} is strictly increasing. Therefore, there exists a positive constant τ_{v_qi} such that $\frac{\partial T_{v_qi}}{\partial(e_{v_qi}/\rho_{v_qi})} \geq \tau_{v_qi} > 0, i =$

$1, 2, \ldots, n$. Hence, $\Psi_{v_q i} \geq \frac{\tau_{v_q i}}{\rho_{v_q 0 i}} > 0,\ i = 1, \ldots, n$. Thus from (59) we obtain the uniform boundedness of $\varepsilon_{v_q i}, i = 1, 2, \ldots, n$ as follows

$$|\varepsilon_{v_q i}| \leq \frac{a_{v_q}\ \rho_{v_q 0 i}}{\tau_{v_q i}}\ , \qquad i = 1, \ldots, n$$

. Finally, form (45) we conclude that $\dot{\varepsilon}_{v_q} \in \mathcal{L}_\infty$, which together with (11) implies $\theta_r(t), \dot{\theta}_r(t) \in \mathcal{L}_\infty$.

Step 3 (ε_θ-subsystem): In Step 3 we consider (46) and the positive definite and radially unbounded Lyapunov function candidate $V_3 = \frac{1}{2}\ \varepsilon_\theta^{\mathsf{T}} \varepsilon_\theta$. Following the same line of proof as in Step 1 we conclude the uniform ultimate boundedness of $\|\varepsilon_\theta\|$ (and thus its uniform boundedness) with respect to the set $\mathcal{E}_\theta = \left\{ \|\varepsilon_\theta\| \in \Re : \|\varepsilon_\theta(t)\| \leq \frac{\sqrt{c_\theta}}{2\kappa_\theta} \right\}$, where $c_\theta = \sup_t \|\rho_{v_\theta} T_{v_\theta}^{-1}(\varepsilon_{v_\theta}) - \dot{\theta}_r - \nu_\theta(\varepsilon_\theta, t)\|^2 > 0$ of the proven bounded term $\|\rho_{v_\theta} T_{v_\theta}^{-1}(\varepsilon_{v_\theta}) - \dot{\theta}_r - \nu_\theta(\varepsilon_\theta, t)\|^2$. As a result we have proved as well the boundedness of Ψ_θ, while $\Psi_\theta^{-1}(\varepsilon_q)$ defined in (8), is bounded by construction. Finally, (46) yields the boundedness of $\dot{\varepsilon}_\theta(t)$, which together with (10) leads to the boundedness of $v_\theta(t), \dot{v}_\theta(t)$.

Step 4 ($\varepsilon_{v_\theta}, \varepsilon_{v_k}$-subsystems): In the final step, the two transformed motor velocity tracking error dynamics (47), (48) are considered, together with the positive definite and radially unbounded Luapunov function candidate $V_4 = \frac{1}{2} \sum_{i \in \{\theta, k\}} \varepsilon_{v_i}^{\mathsf{T}} \varepsilon_{v_i}$. Following the arguments of Step 1, the time derivative of V_4 along (48), (47) yields

$$\begin{aligned} \dot{V}_4 \leq & -\sum_{i \in \{\theta,k\}} \kappa_{v_i} \lambda_{J_i} \lambda_{K_i} \|\varepsilon_{v_i}\|^2 - \sum_{i \in \{\theta,k\}} \kappa_{v_i} \lambda_{J_i} \lambda_{K_i} \|\Psi_{v_i} \varepsilon_{v_i}\|^2 \\ & + \sum_{i \in \{\theta,k\}} \|\varepsilon_{v_i}^{\mathsf{T}} \Psi_{v_i}\| \|\mathcal{B}_{v_i}\| \end{aligned}$$

where $\lambda_{J_i} = \lambda_{\min}(J_i^{-1})$, $\lambda_{K_i} = \lambda_{\min}(K_i)$, $i \in \{\theta, k\}$ and

$$\begin{aligned} \mathcal{B}_{v_i} \ = \ & -\mathcal{Z}_i(\varepsilon_\theta, \varepsilon_{v_\theta}, t) - \mathcal{Z}_{E_i}(\varepsilon_{\theta_k}, \varepsilon_\theta, \varepsilon_q, \varepsilon_{v_q}, t) \\ & -\dot{v}_i - \nu_{v_i}(\varepsilon_{v_\theta}, t), \qquad i \in \{\theta, k\}\ . \end{aligned} \tag{60}$$

Completing the squares we obtain

$$\dot{V}_4 \leq -\sum_{i \in \{\theta,k\}} \kappa_{v_i} \lambda_{J_i} \lambda_{K_i} \|\varepsilon_{v_i}\|^2 + \sum_{i \in \{\theta,k\}} \frac{\|\mathcal{B}_{v_i}\|^2}{4\kappa_{v_i} \lambda_{J_i} \lambda_{K_i}}.$$

To proceed we need to show the boundedness of $\|\mathcal{B}_{v_i}\|$, $i \in \{\theta, k\}$ defined in (60). In Steps 1, 2, 3 we have proved the boundedness of $\varepsilon_q, \varepsilon_{\theta_k}, \varepsilon_\theta, \varepsilon_{v_q}$. Moreover $\nu_{v_\theta}(\varepsilon_{v_\theta}, t)$ and $\nu_{v_k}(\varepsilon_{v_k}, t)$ are bounded by construction. Additionally owing to (4), (28), (32), (38), (39), (40), (41) the terms $\mathcal{Z}_\theta(\varepsilon_\theta, \varepsilon_{v_\theta}, t)$, $\mathcal{Z}_{E_\theta}(\varepsilon_{\theta_k}, \varepsilon_\theta, \varepsilon_q, \varepsilon_{v_q}, t)$, $\mathcal{Z}_{\theta_k}(\varepsilon_{\theta_k}, \varepsilon_{v_k}, t)$ and $\mathcal{Z}_k(\varepsilon_{\theta_k}, \varepsilon_\theta, \varepsilon_q, \varepsilon_{v_q}, t)$ are proven bounded. Therefore, all terms appearing in (60) are bounded, which directly leads to the boundedness of $\|\mathcal{B}_{v_i}\|$, $i \in \{\theta, k\}$. If we denote by $c_{v_i} = \sup_t \|\mathcal{B}_{v_i}\|^2 > 0\ , i \in \{\theta, k\}$, $\dot{V}_4$ becomes:

$$\dot{V}_4 \leq -\sum_{i \in \{\theta,k\}} \kappa_{v_i} \lambda_{J_i} \lambda_{K_i} \|\varepsilon_{v_i}\|^2 + \sum_{i \in \{\theta,k\}} \frac{c_{v_i}}{4\kappa_{v_i} \lambda_{J_i} \lambda_{K_i}}. \tag{61}$$

From (61) we conclude the uniform ultimate boundedness of ε_{v_i}, $i \in \{\theta, k\}$ with respect to the sets $\mathcal{E}_{v_i} = \left\{ \|\varepsilon_{v_i}\| \in \mathbb{R} : \|\varepsilon_{v_i}(t)\| \leq \frac{\sqrt{c_{v_i}}}{2\kappa_{v_i} \lambda_{J_i} \lambda_{K_i}} \right\}$, $i \in \{\theta, k\}$ and consequently their uniform boundedness. Finally, owing to (47), (48), $\dot{\varepsilon}_{v_i}(t)\ , i \in \{\theta, k\}$ are also bounded.

Summarizing, the controller (9)-(14) proves the uniform boundedness of the transformed errors ε_q, ε_{θ_k}, ε_{v_q}, ε_θ, ε_{v_θ}, ε_{v_k}, thus solving the PPC/VSA problem.

ACKNOWLEDGMENT

The authors would like to thank Dr. N.G. Tsagarakis for introducing them to the problem of VSA robot control and provide access to VSA model data.

REFERENCES

[1] J. Choi, S. Park, W. Lee, and S. . Kang, "Design of a robot joint with variable stiffness," in *IEEE International Conference on Robotics and Automation*, 2008, pp. 1760–1765.

[2] S. Wolf and G. Hirzinger, "A new variable stiffness design: Matching requirements of the next robot generation," in *IEEE International Conference on Robotics and Automation*, 2008, pp. 1741–1746.

[3] N. G. Tsagarakis, I. Sardellitti, and D. G. Caldwell, "A new variable stiffness actuator (CompAct-VSA): Design and modelling," in *IEEE International Conference on Intelligent Robots and Systems*, 2011, pp. 378–383.

[4] R. Carloni, L. C. Visser, and S. Stramigioli, "Variable stiffness actuators: A port-based power-flow analysis," *IEEE Transactions on Robotics*, vol. 28, no. 1, pp. 1–11, 2012.

[5] A. Bicchi and G. Tonietti, "Fast and soft arm tactics: Dealing with the safety-performance tradeoff in robots arm design and control," *IEEE Robotics and Automation Magazine*, vol. 11, no. 2, pp. 22–33, 2004.

[6] M. Catalano, G. Grioli, M. Garabini, F. Bonomo, M. Mancinit, N. Tsagarakis, and A. Bicchi, "VSA-CubeBot: A modular variable stiffness platform for multiple degrees of freedom robots," in *IEEE International Conference on Robotics and Automation*, 2011, pp. 5090 – 5095.

[7] R. Schiavi, G. Grioli, S. Sen, and A. Bicchi, "VSA-II: A novel prototype of variable stiffness actuator for safe and performing robots interacting with humans," in *IEEE International Conference on Robotics and Automation*, 2008, pp. 2171–2176.

[8] F. Flacco and A. De Luca, "Stiffness estimation and nonlinear control of robots with variable stiffness actuation," in *18th IFAC World Congress*, Milano, Italy, Aug. 2011, pp. 6872 – 6879.

[9] G. Palli, C. Melchiorri, and A. De Luca, "On the feedback linearization of robots with variable joint stiffness," in *IEEE International Conference on Robotics and Automation*, 2008, pp. 1753–1759.

[10] G. Palli and C. Melchiorri, "Robust control of robots with variable joint stiffness," in *International Conference on Advanced Robotics*, 2009.

[11] ——, "Task space control of robots with variable stiffness actuation," in *IFAC Symposium on Nonlinear Control Systems*, 2010, pp. 1205–1210.

[12] A. Albu-Schaeffer, S. Wolf, O. Eiberger, S. Haddadin, F. Petit, and M. Chalon, "Dynamic modelling and control of variable stiffness actuators," in *IEEE International Conference on Robotics and Automation*, 2010, pp. 2155–2162.

[13] F. Petit and A. Albu-Schaeffer, "State feedback damping control for a multi dof variable stiffness robot arm," in *IEEE International Conference on Robotics and Automation*, 2011, pp. 5561 – 5567.

[14] R. Ozawa and H. Kobayashi, "A new impedance control concept for elastic joint robots," in *Robotics and Automation, 2003. Proceedings. ICRA '03. IEEE International Conference on*, vol. 3, 2003, pp. 3126–3131 vol.3.

[15] I. Sardellitti, G. A. Medrano-Cerda, N. G. Tsagarakis, A. Jafari, and D. G. Caldwell, "Gain scheduling control for a class of variable stiffness actuators based on lever mechanisms," *IEEE Transactions on Robotics*, vol. 29, no. 3, pp. 791–798, Jun. 2013.

[16] A. DeLuca, F. Flacco, A. Bicchi, and R. Schiavi, "Nonlinear decoupled motion-stiffness control and collision detection/reaction for the VSA-II variable stiffness device," in *IEEE/RSJ International Conference on Intelligent Robots and Systems*, 2009, pp. 5487 – 5494.

[17] E. Psomopoulou, Z. Doulgeri, G. A. Rovithakis, and N. G. Tsagarakis, "A simple controller for a variable stiffness joint with uncertain dynamics and prescribed performance guarantees," in *IEEE/RSJ International Conference on Intelligent Robots and Systems*, Oct. 2012, pp. 5071–5076.

[18] A. K. Kostarigka, Z. Doulgeri, and G. A. Rovithakis, "Prescribed performance tracking for flexible joint robots with unknown dynamics and variable elasticity," *Automatica*, vol. 49, no. 5, pp. 1137 – 1147, 2013.

[19] S. Heshmati-alamdari, C. Bechlioulis, M. Liarokapis, and K. J. Kyriakopoulos, "Prescribed performance image based visual servoing under field of view constraints," in *IEEE/RSJ International Conference on Intelligent Robots and Systems*, 2014.

[20] Y. Karayiannidis and Z. Doulgeri, "Model-free robot joint position regulation and tracking with prescribed performance guarantees," *Robotics and Autonomous Systems*, vol. 60, no. 2, pp. 214 – 226, 2012.

[21] ——, "Regressor-free prescribed performance robot tracking," *Robotica*, vol. 31, pp. 1229–1238, 12 2013.

[22] C. Bechlioulis, M. Liarokapis, and K. J. Kyriakopoulos, "Robust model free control of robotic manipulators with prescribed transient and steady state performance," in *IEEE/RSJ International Conference on Intelligent Robots and Systems*, 2014.

[23] A. Atawnih, D. Papageorgiou, and Z. Doulgeri, "Reaching for redundant arms with human-like motion and compliance properties," *Robotics and Autonomous Systems*, vol. 62, no. 12, pp. 1731 – 1741, 2014.

[24] Y. Karayiannidis and Z. Doulgeri, "Regressor-free robot joint position tracking with prescribed performance guarantees," in *Robotics and Biomimetics (ROBIO), 2011 IEEE International Conference on*, Dec 2011, pp. 2312–2317.

[25] G. Karras, C. Bechlioulis, S. Nagappa, N. Palomeras, K. J. Kyriakopoulos, and M. Carreras, "Motion control for autonomous underwater vehicles: A robust model - free approach," in *IEEE International Conference on Robotics and Automation*, 2014.

[26] C. Bechlioulis, G. Karras, S. Nagappa, N. Palomeras, K. Kyriakopoulos, and M. Carreras, "A robust visual servo control scheme with prescribed performance for an autonomous underwater vehicle," in *Intelligent Robots and Systems (IROS), 2013 IEEE/RSJ International Conference on*, Nov 2013, pp. 3879–3884.

[27] P. Marantos, C. Bechlioulis, and K. J. Kyriakopoulos, "Robust stabilization control of unknown small-scale helicopters," in *IEEE International Conference on Robotics and Automation*, 2014.

[28] C. P. Bechlioulis and G. A. Rovithakis, "Robust adaptive control of feedback linearizable MIMO nonlinear systems with prescribed performance," *IEEE Transactions on Automatic Control*, vol. 53, no. 9, pp. 2090–2099, 2008.

[29] ——, "Adaptive control with guaranteed transient and steady state tracking error bounds for strict feedback systems," *Automatica*, vol. 45, no. 2, pp. 532 – 538, 2009.

[30] ——, "Prescribed performance adaptive control for multi-input multi-output affine in the control nonlinear systems," *IEEE Transactions on Automatic Control*, vol. 55, no. 5, pp. 1220–1226, May 2010.

[31] ——, "Robust partial-state feedback prescribed performance control of cascade systems with unknown nonlinearities," *IEEE Transactions on Automatic Control*, vol. 56, no. 9, pp. 2224–2230, Sept 2011.